

A&amp;A manuscript no.

(will be inserted by hand later)

Your thesaurus codes are:

03(03.04.1; 07.09.1; 07.19.1: 09.13.1; 20.01.2)

ASTRONOMY  
AND  
ASTROPHYSICS  
10.10.2018

# Extragalactic Large-Scale Structures behind the Southern Milky Way. – II. Redshifts Obtained at the SAAO in the Crux region

A.P. Fairall<sup>1</sup>, P.A. Woudt<sup>1</sup>, and R.C. Kraan-Korteweg<sup>2</sup><sup>1</sup> Department of Astronomy, University of Cape Town, Rondebosch, 7700 South Africa<sup>2</sup> Observatoire de Paris, DAEC, Unité associée au CNRS, D0173, et à l'Université Paris 7, 92195 Meudon Cedex, France

Received date; Accepted date

**Abstract.** In our systematic optical galaxy search behind the southern Milky Way, 3760 (mostly unknown) galaxies with diameters  $D \gtrsim 0.2'$  were identified in the Crux region ( $287^\circ \lesssim \ell \lesssim 318^\circ$ ,  $|b| \lesssim 10^\circ$ , Woudt & Kraan-Korteweg 1997). Prior to this investigation, only 65 of these galaxies had known redshifts. In order to map the galaxy distribution in redshift space we obtained spectra for 226 bright ( $B_J \lesssim 18$ ) objects with the 1.9m telescope of the South African Astronomical Observatory (SAAO).

Redshifts could be determined for 209 objects, of which 173 have good signal-to-noise ratios. Of the 36 tentative redshifts, four are confirmed through independent values in the literature. The redshifts of three objects indicate them to be galactic of origin. One of these confirms a suspected Planetary Nebula. For 17 of the galaxies, no redshift could be determined due to poor signal-to-noise ratios.

In addition, 26 redshifts have been measured in the Hydra–Antlia region investigated earlier (Kraan-Korteweg, Fairall & Balkowski 1995), of which one is a tentative estimate.

Two main structures crossing the Galactic Plane in the Crux region have now become clear. A narrow, nearby filament from  $(\ell, b) = (340^\circ, -25^\circ)$  to the Centaurus cluster can be traced. This filament runs almost parallel to the extension of the Hydra–Antlia clusters found earlier and is part of what we have earlier termed the “Centaurus Wall” extending in redshift-space between  $0 \leq v \leq 6000$  km s $^{-1}$  (Fairall & Paverd 1995). The main outcome of this survey however, is the recognition of another massive extended structure between  $4000 \leq v \leq 8000$  km s $^{-1}$ . This broad structure, dubbed the Norma Supercluster (Woudt et al. 1997), runs nearly parallel to the Galactic Plane from Vela to ACO 3627 (its centre) from where it continues to the Pavo cluster. This massive structure is believed to be associated with the Great Attractor.

---

Send offprint requests to: A.P. Fairall

The survey has furthermore revealed a set of cellular structures, similar to those seen in redshift space at higher galactic latitudes, but never before seen so clearly behind the Milky Way.

---

**Key words:** redshifts of galaxies – clustering of galaxies – zone of avoidance – large-scale structure of the Universe

## 1. Introduction

This paper is the second in a series reporting redshifts for galaxies found at very low galactic latitudes, obtained for the purpose of mapping large-scale structures previously hidden by the southern Milky Way. The first paper (Kraan-Korteweg, Fairall & Balkowski 1995 - hereafter Paper I) dealt with the Hydra–Antlia region; it also gave full details of the nature of the survey. The present paper covers the “Crux” region immediately neighbouring Hydra–Antlia; it does not repeat information given in Paper I, to which the reader is referred for an extensive description of the motivation, survey and observing procedures.

As before, galaxies in the general galactic latitude range  $|b| \lesssim 10^\circ$  have been found by scanning film copies of the SRC IIIaJ survey under 50 times magnification, the details of which will be presented as a catalogue (Woudt & Kraan-Korteweg 1997, hereafter WK97). For the present work, some 500 square degrees of sky has been searched. It involves 21 fields limited at  $|b| = 10^\circ$ , namely F62-67, F94-98, F130-134 and F171-175.

Figure 1 shows the distribution of the 3760 galaxies found in the Crux region. Only  $\sim 2.3\%$  (= 87) of these galaxies had been catalogued before by Lauberts (1982). The entire area surveyed so far by us is indicated in Figure 1. The dashed line on the right demarcates the Hydra–Antlia region, the middle section (solid line) is the Crux

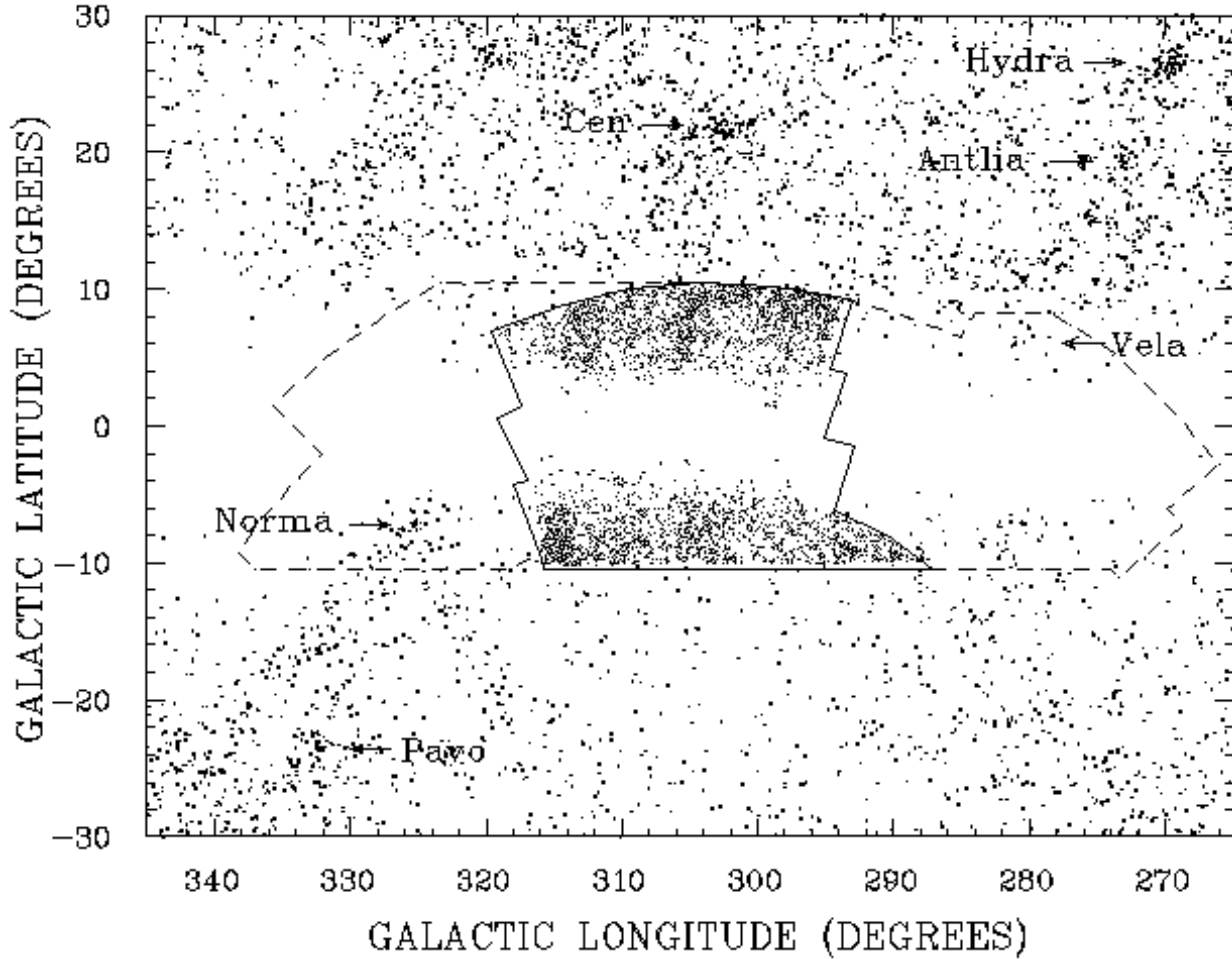


**Fig. 1.** The distribution in Galactic coordinates of the galaxies in the Crux area. The surveyed area is indicated and the newly identified galaxies with  $D \geq 0.2$  arcminutes entered as small dots. The larger dots in the surrounding area display the Lauberts galaxies ( $D \geq 1.0'$ ). The Hydra, Antlia, Centaurus, Pavo and ACO 3627 (=Norma) clusters are labelled, as is the position of the Vela overdensity (reported in Paper I).

region whereas the dashed line on the left shows the Great Attractor region.

The newly found galaxies in the Crux region significantly reduce the width of the “Zone of Avoidance” (ZOA) created by the Milky Way. Nevertheless there is a generally sharp cutoff along the northern boundary at  $b = +3^\circ$  and a more gradual but irregular extinction between  $b = -3^\circ$  and  $-5^\circ$  on the southern edge. The forthcoming blind HI-survey with the multi-beam system at Parkes should unveil the remaining parts of the extragalactic sky between these boundaries.

The distribution of optically detected galaxies inside the Crux region is far from smooth. North of the Milky Way, there are three apparent concentrations at galactic longitudes  $\ell = 296^\circ, 305^\circ$  and  $313^\circ$ . The latter two suggest a continuation of the Centaurus Wall into the ZOA. South of the Milky Way, there is a concentration (at  $\ell = 315^\circ$ )

which is most likely a distant overdensity as the survey reveals a corresponding excess of smaller fainter galaxies.

The Crux region does include part of the “Great Attractor” (GA) (Lynden-Bell et al. 1987). However, the main component of the GA lies within the boundaries of our neighbouring search area ( $318^\circ \lesssim \ell \lesssim 340^\circ, |b| \lesssim 10^\circ$ ) including the centre of the GA which Kolatt et al. (1995) predict at  $\ell = 320^\circ, b = 0^\circ$ . That region will be covered in a third paper in this series; it is dominated by ACO 3627 – hereafter named the Norma cluster – already recognised as a nearby massive cluster (Kraan-Korteweg et al. 1996 – hereafter KK96) while work on this survey was in progress.

## 2. Observations

As before, spectroscopic observations of the more widespread brighter ( $B_J \lesssim 18$ ) galaxies, identified in our survey, have been carried out with the 1.9 m Radcliffe reflector and UNIT Spectrograph at the South African As-

tronical Observatory during four weeks in 1993 – 1995, and are reported in Section 2 below. We have also continued to complement these observations by programmes using the MEFOS (multi-fibre) spectrograph system (Felenbok et al. 1997) on the 3.6m telescope at the European Southern Observatory (for fainter distant galaxies), and using the Parkes radio telescope (to cope with nearby galaxies of low optical brightness). The outcome of these complementary programmes will be presented separately.

The observations at SAAO were carried out over 3500 – 7000Å with a resolution of  $\sim 3\text{\AA}$  per pixel. Integration times typically range from 500 to 2500 seconds. The procedures used for observations, and the reductions carried out thereafter at the University of Cape Town, are the same as described in Paper I.

The entries in Table 1 are as follows:

**Column 1 and 2:** Identification of the galaxy as given in WKK97 and Lauberts identification (Lauberts, 1982).

**Column 3 and 4:** Right Ascension and Declination (1950.0). The positions were measured with the Optronics machine at the ESO in Garching and have an accuracy of about 1 arcsec.

**Column 5 and 6:** Galactic longitude  $\ell$  and latitude  $b$ .

**Column 7:** Large and small diameters (in arcsec). The diameters are measured approximately to the isophote of 24.5 mag arcsec $^{-2}$  and have a scatter of  $\sigma \approx 4''$ .

**Column 8:** Apparent magnitude  $B_J$ . The magnitudes are estimates from the film copies of the SRC IIIaJ Survey based on the above given diameters and an estimate of the average surface brightness of the galaxy. The magnitudes and diameters in the Crux region are estimated by PAW but show no significant deviation from the magnitude and diameter estimates in the Hydra–Antlia region as determined by RCKK (Paper I and Table 2). A more detailed discussion on this subject will follow in WKK97.

**Column 9:** Morphological type. The morphological types are coded similarly to the precepts of the Second Reference Catalogue (de Vaucouleurs *et al.* 1976). Due to the varying foreground extinction a homogeneous and detailed type classification could not always be accomplished and some codes were added: In the first column F for E/S0 was added to the normal designations of E, L, S and I. In the fourth column the subtypes E, M and L are introduced next to the general subtypes 0 to 9. They stand for early spiral (S0/a–Sab), middle spiral (Sb–Sd) and late spiral or irregular (Sdm–Im). The cruder subtypes are a direct indication of the fewer details visible in the obscured galaxy image. The questionmark at the end marks uncertainty of the main type, the colon uncertainty in the subtype.

**Column 10 and 11:** Heliocentric velocity ( $cz$ ) and error as derived from the absorption features. The errors may appear large as they are estimated external errors, and not internal errors (see Paper I). The square brackets indicate a tentative redshift.

**Column 12 and 13:** Heliocentric velocity and error measured from the emission lines (identified in column 14) when present. The square brackets indicate a tentative redshift.

**Column 14:** Identified emission lines:

1	2	3	4	5	6	7
[OII]	H $\gamma$	H $\beta$	[OIII]	[OIII]	H $\alpha$	[NII]
3727	4340	4861	4959	5007	6563	6584

A colon indicates the identification is tentative.

**Column 15:** Code for additional remarks:

1 – WKK 150: The redshift measured at the SAAO for this galaxy is in disagreement with the value quoted in the literature ( $v = 8948 \pm 40 \text{ km s}^{-1}$ , Fisher et al. 1995). It might be due to an identification error; a neighbouring galaxy (WKK 158) was found to be in good agreement with the value quoted in the literature.

2 – The redshifts for these galaxies are tentative only, but confirmed by independent redshifts from the literature.

Sy2 – These four galaxies have been classified as Seyfert 2.

PN – WKK P8: This object was classified as a possible PN, but was not listed in PNe list of Acker 1992. It has now been confirmed as a PN.

Gal – Identification as galaxy questionable, spectra indicates a galactic origin.

\* – Redshifts are also available in the literature.

Table 2 represents an addendum to our Paper I, giving further redshift measurements for galaxies in the Hydra–Antlia region. The format is the same as for Table 1 and the entries in Table 2 are as in Table 1 with the exception of:

**Column 1:** Identification of the galaxy as given in Kraan-Korteweg (1997) for galaxies with the prefix KK, or from Salem & Kraan-Korteweg (1997) for galaxies with the prefix SKK.

**Column 8:** Apparent magnitude  $B_J$  as determined by RCKK. These values are derived similar to the ones quoted in Paper I.

**Column 15:** Code for additional remarks:

3 – KK1196: The redshift measured at the SAAO for this galaxy is in slight disagreement with the value quoted in the literature ( $v = 2411 \text{ km s}^{-1}$ , Huchmeier & Richter 1989).

4 – L216- 5: The redshift measured at the SAAO for this galaxy is in slight disagreement with the value quoted in the literature ( $v = 6350 \text{ km s}^{-1}$ , Visvanathan & v.d. Bergh 1992).

# – These galaxies are not in our search area, but do lie in the “Zone of Avoidance”. The diameters and type are from Lauberts 1982.

### Special cases:

**Table 1.** Galaxies with redshifts obtained at S.A.A.O. in the Crux Region.

Ident.	Laub. Ident.	R.A. (h m s)	Dec. (° ' '')	Long. (°)	Lat. (°)	D x d (")	$B_J$ (mag)	Type	$v_{\text{abs.}}$ (km/s)	err.	$v_{\text{em.}}$ (km/s)	err.	Em.lines	Rm.
(1)	(2)	(3)	(4)	(5)	(6)	(7)	(8)	(9)	(10)	(11)	(12)	(13)	(14)	(15)
WKK 5	L062- 5	10 16 29.3	-68 17 24	289.60	-9.74	73x 15	15.8	S 1	6078	116				
WKK 63		10 37 12.4	-68 30 05	291.36	-8.93	23x 15	17.1	F	17693	109				
WKK 65		10 38 38.6	-69 45 06	292.09	-9.95	35x 11	16.9	S 1			7545	50	1 3 4 5 6	
WKK 80		10 42 39.6	-68 55 19	292.00	-9.06	65x 35	15.1	S 1	9606	132				
WKK 86		10 45 41.3	-67 51 45	291.76	-7.99	23x 16	17.2	S 1	15543	300				
WKK 98		10 48 26.6	-69 11 24	292.59	-9.06	35x 28	16.2	SY 2	17326	160				
WKK 114		10 50 35.6	-69 06 32	292.73	-8.90	19x 13	17.3	E	9382	250	9490	100	6	
WKK 140		10 55 05.0	-70 23 30	293.65	-9.88	27x 19	16.6	F	6417	169	6425	70	6 7	
WKK 149		10 56 21.8	-69 35 52	293.41	-9.12	24x 20	16.8	S 1:	9656	250	9460	70	1 3 6	
WKK 150	L063- 1	10 56 23.7	-69 22 53	293.32	-8.92	77x 31	15.5	S	12005	250	11959	100	6	1
WKK 158	L063- 2	10 57 35.4	-69 26 32	293.44	-8.93	51x 40	15.8	S 5			8768	50	1 3 4 5 6 7	1
WKK 172	L063- 3	10 59 53.6	-70 41 02	294.15	-9.98	83x 47	14.5	S 0:	3848	70				*
WKK 183		11 01 54.0	-70 16 40	294.13	-9.54	32x 11	17.2	S 1	12772	250				
WKK 198		11 05 33.8	-70 09 23	294.37	-9.30	58x 54	15.2	S 2	7716	116				
WKK 213	L063- 8	11 08 22.9	-68 58 11	294.14	-8.11	78x 52	14.8	SB 3	6684	150				
WKK 227	L063-12	11 13 03.5	-67 54 06	294.14	-6.96	60x 52	15.3	S 5:			1328	50	1 3 4 5 6	
WKK 228		11 13 09.1	-67 56 18	294.16	-6.99	34x 27	16.5	I	8233	250				
WKK 235		11 14 12.8	-70 48 47	295.30	-9.64	32x 22	16.6	L	7544	174				
WKK 258		11 20 32.9	-69 10 05	295.23	-7.91	34x 17	16.7	S 1	[13034	220]	[12570	100]	6	2
WKK 269		11 24 29.6	-68 04 06	295.21	-6.75	40x 28	15.9	S 1	5260	177				
WKK 278		11 25 41.6	-70 27 07	296.08	-8.98	39x 11	17.0	S 1			5149	70	3 6	
WKK 284		11 27 53.1	-68 55 46	295.78	-7.47	20x 19	17.3	S ?	7645	250	7708	100	6	
WKK 301	L063-16	11 34 02.3	-70 31 50	296.78	-8.84	69x 38	15.5	S 3:	7769	240	7757	70	6 7	
WKK 315		11 38 29.7	-68 51 05	296.68	-7.12	70x 12	16.5	S 3	7491	103				
WKK 331	L063-19	11 41 39.6	-68 04 56	296.76	-6.30	73x 23	16.1	S 5	12565	250				
WKK 338	L064- 1	11 42 49.5	-71 33 47	297.76	-9.64	70x 23	16.0	S 4	7373	187	7313	100	6	
WKK 354	L064- 2	11 46 32.0	-69 30 54	297.55	-7.58	52x 12	16.8	S 3	7151	235				
WKK 360		11 47 18.2	-68 32 05	297.38	-6.61	35x 26	16.3	L	4111	172				
WKK 370		11 48 34.7	-71 47 26	298.26	-9.75	35x 24	16.7	S			7350	58	3 5 6	
WKK 394	L064- 3	11 50 41.8	-68 19 49	297.64	-6.34	74x 22	15.7	S 0	4137	118				*
WKK 438		11 53 37.7	-68 00 26	297.83	-5.96	36x 19	16.6	S M	[11274	250]				
WKK 485		11 55 29.7	-66 27 31	297.68	-4.41	38x 11	17.2	S	7026	250	6889	70	6 7	
WKK 487	L064- 4	11 55 52.7	-72 06 36	298.89	-9.93	77x 26	15.8	S E	6806	151				
WKK 491	L171- 3	11 56 15.7	-55 02 19	295.44	6.79	73x 15	16.3	S 5	7523	250				
WKK 506		11 57 00.4	-54 40 25	295.47	7.17	27x 19	17.2	S 1	7403	173				
WKK 516		11 57 31.4	-57 15 10	296.06	4.65	27x 9	17.5	L	7338	149				
WKK 540		11 58 46.8	-52 45 23	295.34	9.10	19x 15	17.3	L	14993	107				
WKK 544		11 59 12.5	-52 39 24	295.39	9.21	19x 17	17.1	F	11060	127				
WKK 548		11 59 20.4	-52 38 46	295.41	9.22	22x 16	17.1	L	8320	250	8103	58	3 6 7	
WKK 571		12 00 44.9	-52 35 17	295.61	9.32	19x 12	17.4	E	12141	180				
WKK 576		12 01 42.1	-52 21 14	295.71	9.58	36x 20	16.5	L	14617	250				
WKK 588		12 02 00.9	-52 20 26	295.75	9.60	24x 9	17.8	S 0	8184	182	8172	58	1 5 6	
WKK 589		12 02 02.8	-52 20 06	295.76	9.61	19x 8	17.9	F	8029	250	8044	100	1 6	
WKK 591		12 02 14.3	-52 23 54	295.80	9.55	16x 11	17.7	E	8316	108				
WKK 593	L171- 9	12 02 23.6	-52 57 28	295.92	9.00	55x 9	17.0	S 5:	4609	300	4817	100	6	
WKK 602		12 02 37.9	-72 04 31	299.40	-9.80	20x 8	18.1	L	11724	184				
WKK 627		12 03 54.7	-53 34 52	296.26	8.43	27x 27	16.6	L	8301	148				
WKK 643		12 04 48.0	-52 56 41	296.28	9.08	16x 12	17.5	E	11884	190				
WKK 662	L171-11	12 05 58.7	-53 49 17	296.61	8.25	55x 8	17.0	S 4	[6526	231]				
WKK 708	L171-13	12 08 11.1	-52 34 41	296.73	9.53	91x 8	16.5	S 5	1326	243				
WKK 710		12 08 13.6	-55 04 02	297.14	7.07	40x 27	15.9	SY 4	10409	250				
WKK 728		12 09 11.9	-56 37 50	297.52	5.55	39x 20	16.6	L	7597	210				
WKK 753		12 10 22.1	-52 15 57	297.02	9.89	24x 16	16.8	E	8164	108				
WKK 768		12 11 00.6	-56 02 06	297.68	6.17	22x 16	17.0	L	7740	250	8190	100	6	*
WKK 770		12 11 03.7	-71 09 09	299.91	-8.78	13x 13	18.0	L	[6607	250]				
WKK 783		12 11 29.9	-52 52 29	297.28	9.31	16x 15	17.2	E			16976	100	3 6	
WKK 786		12 11 41.2	-55 11 40	297.65	7.02	46x 28	15.6	L	7518	124				
WKK 828		12 13 52.9	-53 53 12	297.78	8.36	60x 8	16.8	S 5			[7809	100]	6	
WKK 848		12 14 42.2	-53 07 25	297.80	9.13	24x 23	16.9	L	8053	207				
WKK 867		12 15 28.2	-56 27 46	298.36	5.84	47x 35	16.0	L	4076	250				
WKK 868		12 15 29.2	-56 45 58	298.40	5.53	27x 24	16.9	L	8481	250				
WKK 871		12 15 33.0	-70 04 48	300.13	-7.67	27x 8	17.7	S 1	[12717	250]				
WKK 898		12 16 52.0	-56 02 49	298.50	6.27	39x 27	15.8	F	[5855	250]				
WKK 902		12 17 02.2	-53 18 31	298.18	8.99	40x 28	15.6	E 3	5853	113				
WKK 939		12 19 12.9	-52 34 29	298.42	9.76	20x 12	17.2	E			[11890	100]	6	
WKK 959		12 19 59.5	-54 04 38	298.71	8.28	50x 19	15.9	S M	5573	207	5396	100	6	
WKK 986		12 21 20.4	-52 31 12	298.74	9.85	23x 16	17.0	S 0:	18322	178				
WKK1041		12 24 39.0	-56 11 34	299.60	6.25	26x 11	17.5	S 0	7360	250				
WKK1045		12 25 03.6	-52 58 09	299.35	9.46	50x 42	15.4	S 3	5268	250				*
WKK1063		12 26 12.3	-68 45 46	300.93	-6.25	20x 17	17.4	S			6163	50	1 3 5 6	

**Table 1.** – continued

Ident.	Laub. Ident.	R.A. (h m s)	Dec. (° ' '')	Long. (°)	Lat. (°)	D x d (")	$B_J$ (mag)	Type	$v_{abs.}$ (km/s)	err.	$v_{em.}$ (km/s)	err.	Em. lines	Rm.
(1)	(2)	(3)	(4)	(5)	(6)	(7)	(8)	(9)	(10)	(11)	(12)	(13)	(14)	(15)
WKK1069	L172- 2	12 26 29.2	-54 28 10	299.70	7.99	32x 15	17.1	S 4	12326	175				
WKK1078	L172- 3	12 27 02.7	-54 05 14	299.75	8.37	74x 16	15.9	S 1	5635	185				
WKK1089	L172- 4	12 28 16.2	-54 51 40	299.99	7.62	85x 54	14.6	I	[3939	150]				
WKK1110	L064- 7	12 29 30.2	-68 03 38	301.17	-5.53	101x 65	14.6	SB 5	[5834	168]				
WKK1111		12 29 36.7	-68 15 46	301.20	-5.73	36x 28	16.2	L	5270	143				
WKK1169		12 33 22.6	-54 44 04	300.73	7.80	38x 26	16.4	L			4274	70	3 5 6 7	*
WKK1184	L065- 1	12 34 05.2	-72 19 02	301.85	-9.75	34x 23	16.3	E	7100	183				
WKK1209		12 35 21.2	-69 06 00	301.78	-6.53	32x 13	17.3	S 2			5302	50	1 4 5 6	
WKK1218		12 35 57.0	-56 30 09	301.19	6.05	31x 11	17.1	L	5211	250	5159	70	3 6	
WKK1219		12 35 58.7	-72 12 06	301.99	-9.63	30x 9	17.6	S 4	7032	237				
WKK1226		12 36 20.8	-53 50 57	301.11	8.70	51x 20	16.2	S			9424	58	3 4 5 6	
WKK1235		12 37 01.9	-67 43 16	301.86	-5.15	28x 8	17.6	F			6003	100	4 5	
WKK1259		12 38 09.8	-57 31 45	301.54	5.04	20x 16	17.5	L	7242	250				
WKK1263		12 38 33.7	-57 33 36	301.60	5.01	23x 16	17.4	S 1			7324	58	4 5 6	Sy2
WKK1314		12 41 27.9	-68 55 29	302.32	-6.33	30x 16	17.0	S 3	[18844	232]				
WKK1329		12 41 58.1	-72 34 19	302.47	-9.98	47x 20	16.6	S P3			6862	50	1 3 4 5 6	
WKK1352	L172- 8	12 43 19.5	-56 27 59	302.21	6.12	67x 42	15.2	SY 4:			[5528	100]	6	2
WKK1362		12 43 55.7	-52 50 04	302.22	9.76	28x 16	16.8	E	[7282	242]	[6669	70]	1 5 6	
WKK1379	L172-10	12 44 46.3	-53 16 41	302.36	9.32	58x 46	14.8	E ?	1692	250	1797	41	1 3 4 5 6 7	*
WKK1389		12 45 28.7	-53 35 47	302.47	9.00	24x 19	17.0	F	12722	71				
WKK1508		12 51 51.5	-70 58 18	303.24	-8.37	24x 10	17.7	S 0:	15861	189				
WKK1537		12 53 20.9	-54 35 28	303.64	8.00	32x 8	17.6	S 1	[11001	215]				
WKK1554		12 53 57.2	-57 35 12	303.67	5.01	34x 11	17.0	L	5225	113				
WKK1589		12 55 00.1	-53 02 56	303.91	9.54	20x 17	17.6	S E	8394	182				
WKK1619		12 56 15.0	-55 36 52	304.03	6.97	48x 27	16.5	L	4184	108				
WKK1633		12 56 47.0	-53 33 51	304.17	9.02	20x 13	17.5	E	6849	152				
WKK1639		12 57 06.0	-67 33 04	303.78	-4.96	16x 12	17.9	S E:	[9600	222]				
WKK1642		12 57 07.9	-55 43 01	304.15	6.86	34x 23	16.3	F	4077	150	4154	100	3 6	
WKK1648		12 57 22.8	-69 31 42	303.74	-6.94	22x 11	17.4	L	20960	237				
WKK1697		12 59 28.4	-55 40 55	304.49	6.89	34x 27	16.3	S 3	6277	233				
WKK1701		12 59 34.2	-72 02 19	303.83	-9.46	40x 9	17.8	S 4	[16236	250]				
WKK1716		13 00 21.9	-71 51 16	303.90	-9.27	51x 16	16.5	S 3	7183	250	7205	70	6 7	
WKK1719		13 00 33.3	-52 31 09	304.78	10.04	31x 12	17.3	S 2	[7777	300]	[7726	100]	6	
WKK1733		13 00 55.3	-52 43 02	304.83	9.84	23x 11	17.7	S E	5405	226				
WKK1734		13 00 58.0	-56 08 24	304.68	6.42	28x 15	17.2	S M	6696	205	6592	100	6	
WKK1737		13 01 03.1	-52 37 11	304.86	9.94	52x 13	16.8	S 0:	5361	158				
WKK1738		13 01 04.8	-52 37 45	304.86	9.93	16x 11	17.9	F	5405	138				
WKK1759		13 02 03.4	-57 12 42	304.77	5.34	24x 22	16.5	E	5496	205				
WKK1783	L173- 5	13 03 08.6	-57 17 54	304.92	5.25	19x 7	18.1	S 0			[5911	100]	6	2
WKK1810		13 03 52.3	-52 48 51	305.28	9.72	16x 9	18.0	F	8710	182				
WKK1812		13 03 56.8	-56 57 27	305.05	5.58	27x 23	16.6	F	5642	130				
WKK1814		13 03 59.7	-56 58 28	305.05	5.57	23x 12	17.3	F	6011	167				
WKK1818		13 04 09.0	-56 56 35	305.07	5.60	16x 11	17.7	E	5457	239				
WKK1823		13 04 18.8	-55 50 57	305.16	6.69	22x 20	16.8	S 0	6637	182				
WKK1825		13 04 19.7	-56 50 16	305.11	5.70	19x 15	17.3	E	[6347	223]				
WKK1835		13 04 33.4	-56 48 23	305.14	5.73	31x 15	16.7	S E	6126	224				
WKK1842		13 04 53.4	-55 57 27	305.24	6.57	28x 12	17.5	S E	6662	117				
WKK1847		13 04 58.7	-56 47 32	305.20	5.74	16x 16	17.5	S 0	6431	191	6413	70	6 7	
WKK1849		13 05 08.9	-57 28 18	305.18	5.06	22x 12	17.3	L	5597	152				
WKK1851	L173- 7	13 05 12.3	-53 58 40	305.41	8.55	59x 42	15.4	SY 5	5368	250				
WKK P8		13 07 12.3	-59 29 13	305.31	3.03	13x 13	17.8				28	50	3 4 5 6	PN
WKK1910		13 07 28.4	-57 44 23	305.47	4.77	34x 27	16.3	S 0	6843	121				
WKK1957		13 08 57.5	-65 18 28	305.08	-2.79	19x 13	17.6				107	70	5 6	Gal
WKK1992		13 10 20.3	-57 00 41	305.91	5.47	23x 16	17.0	F	5783	165				
WKK2014		13 11 00.4	-58 16 49	305.90	4.20	28x 23	16.7	S 2:	5782	221				
WKK2024		13 11 44.3	-55 06 32	306.27	7.35	30x 17	17.2	L	3615	174				
WKK2029		13 12 01.4	-58 40 20	306.00	3.79	47x 31	16.2	S M			2355	50	1 5 6 7	
WKK2037		13 12 25.2	-55 37 26	306.33	6.83	34x 12	17.2	S 3:	3579	147				
WKK2043		13 12 42.6	-52 55 58	306.62	9.50	54x 34	15.9	L	3568	159				
WKK2047		13 12 50.3	-55 38 54	306.38	6.80	20x 11	17.8	S E	7068	250				
WKK2068		13 13 41.2	-55 18 44	306.54	7.12	44x 17	16.7	S 0	7011	132				
WKK2084		13 14 35.3	-69 57 31	305.21	-7.47	23x 17	17.0	F	22087	158				
WKK2090		13 14 58.9	-69 55 24	305.24	-7.44	47x 24	16.2	S E	14718	153				
WKK2110		13 16 04.2	-56 48 45	306.72	5.59	13x 9	18.2	E	6064	177				
WKK2143		13 18 37.7	-56 33 41	307.09	5.80	59x 11	16.9	S 4	5369	199				
WKK2156		13 19 32.2	-53 10 20	307.63	9.15	52x 20	16.2	L ?	3805	71				
WKK2160		13 19 45.2	-52 25 42	307.75	9.89	27x 24	16.5				3512	58	1 6 7	
WKK2165		13 19 52.2	-57 16 24	307.18	5.08	13x 9	18.2	L	[5037	230]				
WKK2181		13 20 47.6	-70 29 12	305.67	-8.05	52x 43	15.8	S R	[9045	250]				
WKK2183	L065- 6	13 20 56.8	-70 12 29	305.72	-7.78	87x 51	14.7	SB 5	7157	167				

**Table 1.** – continued

Ident.	Laub. Ident.	R.A. (h m s)	Dec. (° ′ ″)	Long. (°)	Lat. (°)	D x d (")	$B_J$ (mag)	Type	$v_{\text{abs.}}$ (km/s)	err.	$v_{\text{em.}}$ (km/s)	err.	Em. lines	Rm.
(1)	(2)	(3)	(4)	(5)	(6)	(7)	(8)	(9)	(10)	(11)	(12)	(13)	(14)	(15)
WKK2224		13 23 21.6	-53 39 06	308.14	8.61	56x 54	15.8	SYR3		5228	58	3 5 6 7		
WKK2244		13 24 27.5	-55 33 33	308.03	6.69	22x 9	17.8	S 0	5950	201				
WKK2270		13 25 31.8	-71 58 30	305.85	-9.58	24x 10	17.5	S 0:	13950	238				
WKK2303		13 28 29.2	-57 37 47	308.28	4.57	19x 11	18.0	S	[4975	250]				
WKK2334		13 30 24.1	-57 32 20	308.55	4.62	19x 15	17.6	L	5667	159				
WKK2338		13 30 42.6	-57 45 08	308.56	4.40	20x 11	17.9	S 0	5393	250				
WKK2345		13 31 08.9	-52 40 45	309.45	9.39	35x 30	16.8	SBR	14283	141				
WKK2349		13 31 20.8	-71 04 15	306.46	-8.75	60x 34	16.1	S R5	[10085	250]				
WKK2389		13 34 06.0	-69 54 59	306.88	-7.66	16x 11	17.9	S 0			19798	100	5	Sy2
WKK2395		13 34 22.0	-53 04 06	309.87	8.93	31x 13	17.1	S 0	5992	134				
WKK2407		13 35 05.6	-70 00 45	306.95	-7.77	28x 17	16.9	S 1:	20381	132				
WKK2433	L066- 1	13 36 27.2	-70 52 34	306.91	-8.64	78x 44	14.9	S 5			[5214	100]	6	2
WKK2493		13 40 12.7	-71 01 09	307.18	-8.84	36x 30	16.1	S 2			7220	45	1 3 5 6 7	*
WKK2497		13 40 26.0	-56 26 29	310.10	5.45	24x 12	17.4	S E			5241	50	1 4 5 6	
WKK2508		13 41 31.1	-71 03 39	307.28	-8.90	35x 26	16.5	L ?	7165	195	7179	70	5 6	
WKK2519	L066- 2	13 42 33.9	-69 27 26	307.70	-7.35	51x 28	15.8	SB 4	[2071	250]				
WKK2647		13 50 40.1	-53 39 30	312.15	7.85	23x 15	16.8	F			3622	38	1 3 4 5 6 7	
WKK2661		13 51 04.3	-66 42 34	309.09	-4.84	13x 11	18.0	S 0:	11137	162				
WKK2674		13 51 24.2	-54 18 58	312.10	7.18	17x 16	17.3	E	11865	177				
WKK2693	L066- 3	13 52 31.4	-70 40 58	308.25	-8.73	118x 16	15.7	S 5	[7389	250]				
WKK2736	L174- 4	13 54 36.7	-53 46 35	312.69	7.59	98x 22	15.2	L	4321	300				
WKK2764		13 55 29.5	-58 31 27	311.60	2.96	15x 13	18.1	S	3687	184				
WKK2766		13 55 32.4	-66 49 21	309.49	-5.06	20x 11	17.7	L ?	7323	143				
WKK2817		13 57 38.6	-55 29 22	312.67	5.82	31x 24	16.4	L	2860	85				
WKK2868		13 59 08.4	-54 28 09	313.16	6.75	43x 32	16.2	E	4990	101				
WKK2877		13 59 22.6	-54 15 29	313.25	6.94	26x 12	17.3	S 0	2682	199	2687	70	6 7	
WKK2917		14 01 10.5	-69 29 43	309.29	-7.78	47x 23	16.2	SB 5			16803	100	6	
WKK2918		14 01 10.9	-69 30 06	309.29	-7.79	17x 9	17.9	S E			16814	45	1 2 3 4 5 6	
WKK2920		14 01 15.6	-52 27 27	314.02	8.59	48x 16	16.6	S 2	3716	164				
WKK2935		14 01 51.3	-53 25 13	313.83	7.64	19x 12	17.6	L	[9528	196]				
WKK2938		14 01 55.6	-65 26 45	310.49	-3.91	34x 22	16.3	L	3024	157				
WKK2950		14 02 28.6	-53 29 02	313.90	7.56	27x 11	17.6	L	[10127	300]				
WKK2953		14 02 36.1	-53 28 51	313.92	7.55	42x 11	17.2	S	3939	233				
WKK2985		14 04 43.5	-71 33 48	308.98	-9.85	19x 12	17.6	E	16514	182				
WKK2990		14 05 13.3	-56 01 31	313.55	5.01	22x 13	17.3	E			5291	100	6 7	
WKK2993	L175- 3	14 05 17.0	-54 59 54	313.86	5.99	62x 28	15.8	S M			4364	45	1 3 4 5 6	*
WKK3005		14 06 11.3	-56 07 12	313.65	4.88	20x 9	18.2	S E	[11909	241]				
WKK3012	L097-12	14 06 44.6	-65 20 49	311.00	-3.96	67x 20	16.0	S 0	3127	192				
WKK3023		14 07 12.3	-60 04 59	312.61	1.05	43x 15	16.6	S E?	-121	185				Gal
WKK3027		14 07 28.5	-69 40 09	309.77	-8.10	26x 19	17.2	L ?			12360	100	3 6	
WKK3041		14 08 50.6	-70 46 18	309.54	-9.19	47x 28	16.1	S P	7439	241	7604	70	6 7	
WKK3062		14 10 14.8	-70 12 18	309.83	-8.69	30x 16	16.9	F	16777	168				
WKK3083		14 12 11.6	-65 01 08	311.64	-3.82	30x 17	17.0	S	2947	235	2999	70	6 7	
WKK3089		14 12 38.1	-53 29 05	315.36	7.10	31x 14	17.0	L	3836	171				
WKK3091	L221-35	14 12 42.5	-52 22 36	315.72	8.15	83x 27	15.3	S 1	3279	162				
WKK3174		14 21 05.3	-71 11 04	310.36	-9.91	20x 13	17.6	F	16244	138				
WKK3193		14 23 10.0	-52 30 33	317.19	7.48	54x 12	16.8	S 3	[3121	250]				
WKK3209		14 24 40.7	-71 03 59	310.67	-9.90	19x 19	17.3	E	16931	112				
WKK3262		14 30 49.7	-69 30 52	311.75	-8.66	23x 19	16.9	E ?	8013	250	7751	70	5 6	Sy2
WKK3263		14 30 51.4	-69 37 36	311.71	-8.76	31x 20	16.7	L ?	7790	154				
WKK3277		14 32 21.7	-68 48 33	312.16	-8.06	20x 11	17.8	L ?	[14323	250]				
WKK3282		14 33 02.4	-52 27 38	318.62	6.96	27x 15	17.1	E ?	[10682	204]				
WKK3288		14 33 31.1	-53 49 37	318.14	5.68	21x 12	17.5	S E			2928	70	6 7	
WKK3292		14 33 37.6	-53 47 46	318.17	5.70	38x 12	17.4	S M:	[2893	195]				
WKK3297		14 34 03.7	-53 51 45	318.20	5.62	26x 24	16.6	E	2955	115				
WKK3343		14 38 57.9	-67 04 56	313.43	-6.73	36x 12	17.6	S			8767	58	3 6 7	
WKK3346	L067- 3	14 39 12.5	-65 55 05	312.26	-9.32	63x 16	16.4	S 3:			5147	100	6 7	
WKK3374		14 42 30.3	-65 14 22	314.53	-5.21	17x 12	17.7	S ?	14368	156				
WKK3456		14 49 17.0	-70 03 41	312.99	-9.82	36x 23	16.3	E	8051	143				
WKK3465		14 50 11.0	-69 54 59	313.12	-9.73	47x 34	15.8	S 0:	8008	178				
WKK3475		14 50 51.2	-70 01 51	313.12	-9.86	27x 17	17.1	L ?	[23626	194]				
WKK3568		14 56 33.7	-69 55 41	313.61	-9.99	30x 20	16.6	L			8109	58	3 6 7	
WKK3632		14 59 01.9	-68 44 50	314.38	-9.06	15x 12	17.7	E	9801	250				
WKK3646		15 00 08.1	-67 48 26	314.93	-8.29	30x 11	17.3	F			4488	58	1 4 5 6	Sy2
WKK3658		15 00 49.5	-67 32 53	315.11	-8.09	47x 19	16.8	S M	11299	192				
WKK3715		15 06 06.5	-67 42 55	315.47	-8.49	17x 15	17.4	E	15641	168				
WKK3720		15 06 36.2	-68 32 26	315.09	-9.22	23x 15	17.3	F	[19863	233]				
WKK3737	L067- 9	15 09 20.1	-69 01 33	315.05	-9.77	40x 32	15.3	E ?	7781	237				*
WKK3758		15 13 29.7	-68 37 10	315.59	-9.62	56x 34	15.2	S 5	[8672	250]				

**Table 2.** Galaxies with redshifts obtained at S.A.A.O. in the Hydra/Antlia Region, addendum Paper I.

Ident.	Laub. Ident.	R.A. (h m s)	Dec. (° ' '')	Long. (°)	Lat. (°)	D x d (")	$B_J$ (mag)	Type	$v_{\text{abs.}}$ (km/s)	err.	$v_{\text{em.}}$ (km/s)	err.	Em. lines	Rm.
(1)	(2)	(3)	(4)	(5)	(6)	(7)	(8)	(9)	(10)	(11)	(12)	(13)	(14)	(15)
KK 166	L165- 3	08 36 09.7	-57 22 41	273.76	-9.90	74x 16	16.1	S 3	18269	201				*
KK 1159	L126- 3	09 13 23.0	-60 13 30	279.09	-8.03	114x 67	13.5	SB 4	2825	250	2851	100	6 7	
KK 1194	L126- 5	09 16 21.3	-59 24 19	278.76	-7.19	60x 27	15.5	S 4	10166	233	10240	100	6	
KK 1196	L091- 7	09 16 21.9	-62 40 19	281.13	-9.47	121x 81	13.4	S 5	1606	250				3
KK 1265	L126-10	09 21 08.3	-60 50 05	280.21	-7.77	121x 40	14.0	S 3	1992	177	2000	100	6	*
KK 1300	L091-12	09 23 20.9	-63 01 40	281.96	-9.15	74x 63	14.7	S 5	2866	250				
KK 1384	L126-16	09 28 00.5	-60 28 25	280.56	-6.93	81x 38	14.9	S	2086	157				
KK 1492	L126-22	09 35 37.4	-60 42 23	281.41	-6.47	81x 34	14.9	SB 4	2928	227				
SKK1514	L262-15	10 00 38.9	-45 15 26	274.56	7.87	60x 24	15.1	S 1	3235	250	3451	50	3 6 7	*
KK 1907	L092- 6	10 01 54.6	-64 43 26	286.32	-7.67	148x 87	13.5	SXR3	2085	107				*
KK 1938	L062- 2	10 03 59.3	-67 30 14	288.17	-9.78	60x 54	15.1	SX 3			5194	41	1 3 4 5 6 7	
KK 1977		10 06 19.2	-48 58 24	277.55	5.44	20x 13	17.1		18918	234	18864	58	1 3 6	
KK 2043	L092-15	10 09 39.4	-66 53 50	288.26	-8.96	60x 47	15.0	SX 3	5409	157	5204	100	6 7:	
SKK1786	L263-17	10 10 40.7	-45 33 10	276.17	8.66	31x 13	16.7	L	18177	114				
KK 2095		10 11 31.0	-52 16 27	280.12	3.21	40x 20	16.0	S 3	8388	250	8576	70	6 7	
KK 2109	L213- 9	10 11 50.9	-52 02 16	280.03	3.43	47x 40	15.3	SB 3	2553	250	2714	70	6 7	*
KK 2182		10 14 22.0	-67 40 28	289.08	-9.34	40x 15	16.5	S 1			1923	100	1:6 7:	*
SKK1861	L263-27	10 15 52.3	-46 37 40	277.54	8.28	84x 48		L	13270	250				
KK 2443		10 21 44.8	-51 16 42	280.90	4.91	74x 7	17.1	S	[1725	250]				
KK 2505		10 23 57.5	-67 23 55	289.71	-8.61	30x 16	16.8	S E?	5861	206	5792	100	6	
KK 2539		10 25 03.8	-67 25 29	289.81	-8.58	23x 16	17.0	F ?	6253	229	5855	58	3 5 6	
KK 2652	L214-13	10 28 57.0	-48 47 25	280.58	7.63	87x 48	14.5	S 3	4997	250				*
	L215-10	10 56 01	-50 10 30	285.15	8.48	66x 36		L	5898	170				#
	L215-12	10 56 31	-50 03 24	285.18	8.62	132x 24		S 3	2901	250				#*
	L216- 5	11 17 11	-52 05 54	289.00	7.99	126x 66		S 1	5267	99				#4
KK 2991	L170- 2	11 23 43.3	-52 30 16	290.09	7.95	81x 81	14.5	SBR5	5084	250				*

**Table 3.** Galaxies observed at the SAAO without reliable redshift.

Ident.	Laub. Ident.	R.A. (h m s)	Dec. (° ' '')	Long. (°)	Lat. (°)	D x d (")	$B_J$ (mag)	Type	Remarks
(1)	(2)	(3)	(4)	(5)	(6)	(7)	(8)	(9)	(10)
WKK 110		10 50 23.2	-69 06 37	292.71	-8.91	28x 8	17.6	S 0	S/N too low
WKK 199		11 05 34.1	-70 06 25	294.35	-9.26	58x 30	15.9	SY 5	S/N too low
WKK 585	L171- 6	12 01 53.0	-53 39 27	295.98	8.30	87x 11	16.4	S 5	S/N too low
WKK 647		12 05 03.8	-52 58 43	296.33	9.05	31x 16	16.9	S	s.p.* spec.
WKK 819		12 13 25.6	-52 43 02	297.55	9.51	22x 16	17.2	F	No rel.feat.
WKK 919		12 18 19.3	-53 15 10	298.36	9.07	46x 26	15.7	S M	S/N too low
WKK1070	L172- 2	12 26 30.6	-54 28 29	299.70	7.98	35x 8	17.4	S 2:	S/N too low
WKK1179		12 33 54.4	-68 14 25	301.60	-5.68	27x 9	17.9	S 1	No rel.feat.
WKK1324		12 41 52.6	-72 02 59	302.44	-9.46	32x 9	17.6	S E	S/N too low
WKK1501		12 51 35.8	-68 31 56	303.24	-5.93	17x 9	17.8	S 0:	No rel.feat.
WKK1510		12 51 55.2	-55 37 39	303.42	6.97	66x 11	16.6	S 4	S/N too low
WKK1822	L173- 6	13 04 18.1	-53 51 34	305.28	8.67	60x 30	15.9	S R5	S/N too low
WKK1852		13 05 14.4	-54 28 23	305.38	8.05	19x 17	17.1	L	No rel.feat.
WKK2783		13 56 31.2	-56 31 05	312.25	4.87	23x 13	17.2	F	S/N too low
WKK3522		14 54 12.2	-66 16 45	315.15	-6.67	23x 17	17.3	L	S/N too low
WKK3681		15 02 15.7	-67 56 42	315.04	-8.51	43x 27	16.1	SB 3	No rel.feat.
WKK3751		15 12 18.9	-68 29 19	315.57	-9.45	26x 22	16.6		No rel.feat.

In the course of this survey we have given special attention to a number of objects that, based on their optical appearance, might be Planetary Nebulae (PNe). In the Crux region there are four such objects and these observations are described elsewhere (Kraan-Korteweg et al. 1996b): Two of the four PNe candidates were too faint to be detected, one was confirmed as being a PN (PNG 299.5+02.5) and one object was classified as a new PN (PNG 298.3+06.7).

Table 3 lists galaxies for which the spectra has too poor a signal-to-noise ratio for a redshift to be extracted. For one galaxy (WKK 647) the spectrum was dominated by a superimposed foreground star and no reliable redshift could be extracted.

Table 4 lists the galaxies with their optical properties as determined in our Crux survey, for which redshifts have already been published in the literature. Although now reobserved by us, these galaxies clearly would have been included in our observations, since they meet our selec-

**Table 4.** Galaxies in the Crux region with radial velocities from the literature (NED) in the Crux Region.

Ident.	Laub. Ident.	R.A. (h m s)	Dec. (° ' '')	Long. (°)	Lat. (°)	D x d ('')	$B_J$ (mag)	Type	$v_{hel}$ (km/s)	err.	Ref.
(1)	(2)	(3)	(4)	(5)	(6)	(7)	(8)	(9)	(10)	(11)	(12)
WKK 224	L063-11	11 11 10.8	-68 59 39	294.38	-8.04	255x 50	13.6	S 3	1383	1	
WKK 358		11 47 02.2	-68 24 55	297.32	-6.50	58x 9	16.8	S 4	7476	48	2
WKK 399		11 50 53.9	-53 20 11	294.30	8.28	38x 26	16.1	S 1	6718	36	2
WKK 404	L171- 1	11 51 11.8	-53 49 35	294.45	7.81	65x 27	15.9	S 2	6720	3	
WKK 411	L171- 2	11 51 44.4	-53 52 57	294.54	7.78	60x 40	15.6	S R	5359	3	
WKK 475		11 55 01.3	-52 27 39	294.72	9.27	35x 26	16.5	S 5	14716	3	
WKK 496		11 56 26.9	-52 54 42	295.03	8.87	42x 20	16.7	SB 1	9828	3	
WKK 499	L171- 4	11 56 36.6	-53 07 50	295.09	8.67	87x 56	14.5	F	4228	1	
WKK 529		11 58 22.0	-53 34 49	295.45	8.28	12x 11	18.1	E	11700	150	4
WKK 530		11 58 22.6	-53 35 03	295.45	8.27	15x 13	17.7	E	11550	150	4
WKK 543	L171- 5	11 59 02.6	-53 04 44	295.45	8.79	65x 31	15.5	SPR	4276	1	
WKK 560		12 00 13.2	-53 33 26	295.71	8.35	31x 23	16.4	F ?	8384	36	5
WKK 590	L171- 8	12 02 11.3	-52 53 46	295.88	9.06	47x 38	15.4	F	4409	1	
WKK 787		12 11 42.6	-56 15 53	297.81	5.96	20x 17	17.5	L	8141	36	2
WKK 922		12 18 27.4	-52 18 31	298.27	10.01	85x 74	13.7	E 1	4274	1	
WKK 957	L130-12	12 19 54.4	-58 20 20	299.18	4.05	101x 27	15.0	S 2:	1497	1	
WKK1222	L172- 5	12 36 12.7	-53 05 36	301.05	9.46	58x 56	15.3	S 5	8676	1	
WKK1373	L172- 9	12 44 41.2	-53 40 34	302.35	8.92	110x 78	14.1	I ?	1887	1	
WKK1435		12 48 21.7	-53 16 54	302.90	9.32	19x 15	17.4	S	17233	36	5
WKK1576	L172-12	12 54 44.8	-53 07 19	303.87	9.47	94x 54	15.1	S 5	6829	1	
WKK1685		12 58 50.0	-53 49 23	304.47	8.75	22x 16	18.0	S ?	7905	39	2
WKK1698		12 59 29.3	-54 03 40	304.56	8.51	17x 12	17.6	L	8019	39	5
WKK1724	L173- 3	13 00 38.1	-52 49 22	304.78	9.74	87x 55	15.4	S	9850	150	4
WKK1853		13 05 15.0	-57 11 31	305.21	5.34	32x 32	16.3	S 9?	6390	37	2
WKK2031		13 12 02.5	-54 53 32	306.34	7.56	34x 26	16.2	S 1	9222	52	2
WKK2147	L173-11	13 18 53.8	-54 21 04	307.39	7.99	105x 28	15.0	S 5	4153	44	5
WKK2240	L173-15	13 24 11.8	-57 13 48	307.77	5.04	85x 12	16.3	S	3006	36	2
WKK2286		13 26 46.7	-54 24 11	308.53	7.79	87x 71	14.7	SY 4	5224	3	
WKK2287	L173-16	13 26 54.9	-55 18 45	308.42	6.89	90x 59	14.8	S 6	3608	1	
WKK2332	L174- 1	13 30 11.1	-53 05 54	309.24	9.00	141x 91	14.1	L	1382	1	
WKK2363		13 32 05.7	-53 11 03	309.51	8.87	26x 13	17.3	SB 3:	14425	38	2
WKK2375		13 33 17.8	-54 49 30	309.40	7.22	62x 56	15.2	S 5	4290	37	5
WKK2388		13 34 04.7	-54 49 18	309.52	7.21	36x 16	17.0	S 5	3976	40	5
WKK2411		13 35 11.6	-53 38 38	309.89	8.34	22x 9	18.3	S ?	21496	127	5
WKK2523		13 43 01.9	-52 31 39	311.28	9.20	40x 30	16.3	S 5	9185	3	
WKK2575		13 47 14.6	-52 24 47	311.94	9.18	155x 99	13.7	S 5	3674	43	2
WKK2576		13 47 15.2	-52 41 56	311.87	8.90	86x 75	14.6	S 5:	3821	3	
WKK2595		13 48 09.0	-52 40 00	312.01	8.90	102x 40	14.9	S 6	3973	46	2
WKK2609		13 48 56.7	-55 42 47	311.42	5.91	22x 13	17.6		4070	36	2
WKK2670	L174- 2	13 51 17.4	-53 03 58	312.38	8.40	121x 19	15.7	S L	3758	40	5
WKK2730	L174- 3	13 54 18.7	-52 31 42	312.97	8.81	118x 77	14.1	SB 5	4059	37	2
WKK2804		13 57 07.8	-53 28 60	313.13	7.77	34x 32	15.9	S 1	4779	39	5
WKK2863	L174- 5	13 58 54.8	-53 18 01	313.44	7.88	98x 83	14.3	S 5	3775	37	2
WKK2962	L175- 1	14 03 16.6	-55 07 08	313.55	5.96	129x 85	13.8	S 5	3760	1	
WKK2992	L175- 2	14 05 15.2	-53 06 56	314.41	7.79	77x 60	15.1	S R	4062	1	
WKK3050	L097-13	14 09 17.1	-65 06 18	311.32	-3.81	457x155	11.5	S 4	438	9	6
WKK3103		14 13 42.1	-55 18 45	314.92	5.32	161x 23	15.0	S 6	3954	55	2
WKK3139		14 16 55.1	-54 50 22	315.51	5.62	43x 26	15.9	S R	2875	94	5
WKK3249	L175- 9	14 28 26.1	-55 14 45	316.91	4.65	78x 77	14.6	SB 5	3019	1	
WKK3278	L067- 2	14 32 32.4	-70 15 49	311.59	-9.41	74x 17	16.2	S 6	3118	40	5
WKK3491	L067- 4	14 51 46.5	-69 18 11	313.53	-9.25	85x 46	15.0	S 5	8170	1	

tion criteria. Columns 1-9 are the same as in Table 1. Column 10 and 11 list the heliocentric velocities and errors (if given). The velocity in column 10 has been adopted from the source identified in column 12, where the number corresponds to:

1. Dressler 1991, The supergalactic plane redshift survey.
2. Strauss et al. 1992, A redshift survey of IRAS galaxies.
3. Visvanathan & v.d. Bergh 1992, Luminous spiral galaxies in the direction of the Great Attractor.

4. Fairall 1983, Spectroscopic survey of southern compact and bright-nucleus galaxies.
5. Fisher et al. 1995, The IRAS 1.2 Jy Survey.
6. Fairall 1996, The Southern Redshift Catalogue.

### 2.1. Comparison to other measurements

Although the galaxies we observed were initially selected on the basis of having no published redshifts, more recent

publications have provided redshifts from other investigators for 20 of the galaxies in Table 1 and Table 2. This overlap, however, allows a suitable comparison between our sample and others. We find

$$\langle v_{SAAO} - v_{pub} \rangle = +7 \pm 94 \text{ km s}^{-1}$$

which shows no significant systematic error, and agrees well within our average standard deviation.

Similarly, we have allowed a small overlap between the SAAO galaxies and our complementary programmes using Mefos and Parkes radio observations, for which we find

$$\langle v_{SAAO} - v_{MEFOS} \rangle = -49 \pm 118 \text{ km s}^{-1}$$

$$\langle v_{SAAO} - v_{PKS} \rangle = +49 \pm 135 \text{ km s}^{-1}.$$

The comparison with the MEFOS and Parkes data is based on 5 and 12 galaxies respectively. Again, the agreement is acceptable with our standard deviation; the latter in any case probably reflects low surface-brightness galaxies, for which our errors are at their largest values.

### 3. Coverage and Completeness

We have obtained reliable redshifts for 173 galaxies, with tentative redshifts for a further 36 objects, as set out in Table 1. The tentative redshifts are not used in any of the subsequent plots or analyses.

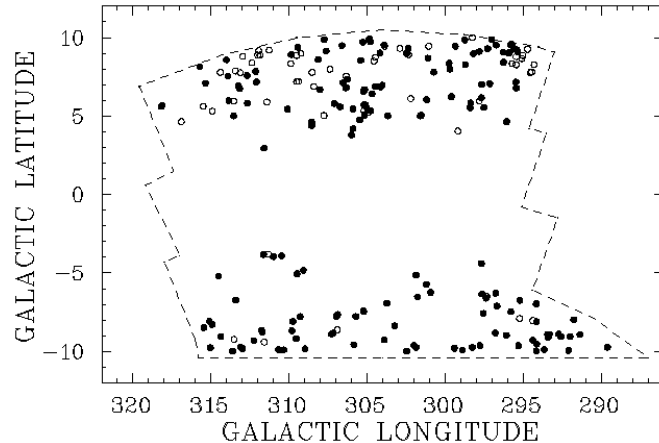


**Fig. 2.** Distribution of the galaxies with radial velocities. The Crux survey region is outlined. Solid circles indicate the positions of galaxies, in the Crux region, observed in the present work, and for which redshifts have been obtained. Open circles show the positions of galaxies for which redshifts are available from the literature.

Figure 2 shows the sky coverage of the galaxies with reliable redshifts, depicted by solid circles. The coverage can be seen to be reasonably uniform, on both the north and south sides of the galactic obscuration. By contrast,

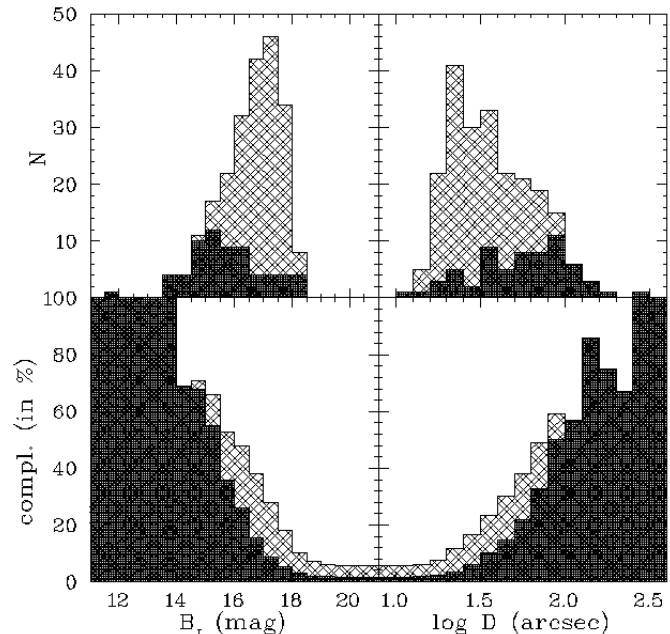


**Fig. 3.** Magnitude and major-axis diameter distribution of galaxies with radial velocities in the Crux search area. The lighter hatched areas mark galaxies observed at the SAAO, the darker hatched by others. The bottom panel shows the completeness in percent of the total number of galaxies found in the Crux Region (cf. fig. 1).

the data from Table 4 – galaxies with previously known redshifts as depicted by the open circles – is strongly concentrated north of the plane. This is due to the redshift surveys in that area that focussed on the Great Attractor (esp. Dressler 1991, Visvanathan & van den Bergh 1992).

Figure 3 presents a comparison of the magnitudes and major-axis distribution of the observed galaxies; it shows general similarity to the corresponding plot in Paper I. The sharp magnitude cut-off indicates the limiting performance of the 1.9m telescope for galaxies fainter than ( $B_J \lesssim 18$ ).

These observations trace the bright end of the magnitude distribution of the 3760 galaxies in the Crux region very well. We are 70% complete for galaxies brighter than ( $B_J \lesssim 14$ ) and even 54% complete for galaxies brighter than ( $B_J \lesssim 16$ ). These numbers are comparable to the completeness figures in the Hydra–Antlia region. As before, a number of bright galaxies are missed by this survey. They are extended low surface brightness spiral galaxies. In the meantime, they have been observed with the Parkes 64-m telescope and will be reported on elsewhere.

## 4. Identification of Large-Scale Structures

### 4.1. Velocity distribution

The histogram of redshifts shown in Figure 4 reveals a broad concentration of galaxies around  $3500 \leq v \leq 8500$

$\text{km s}^{-1}$ , with a probable dip at  $4500 \text{ km s}^{-1}$ . This is quite different to the single peak centred at  $2750 \text{ km s}^{-1}$  for the neighbouring Hydra–Antlia region to the west (Paper I), and the dominating peak at  $4882 \text{ km s}^{-1}$  of the Norma cluster (KK96) to the east. It suggests that quite different large-scale structures may be present in this Crux region, which we shall examine in greater detail below.

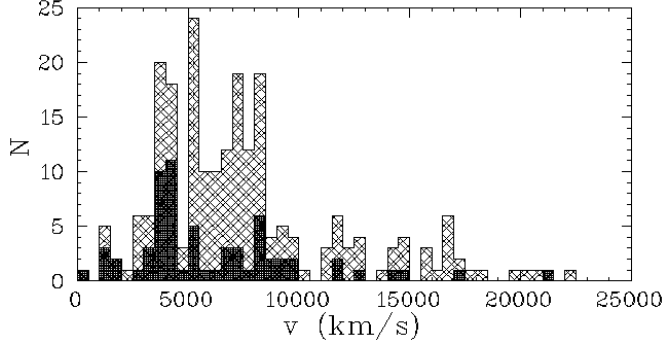


**Fig. 4.** Velocity histogram of the galaxies in the search area in the Crux extension in the ZOA. Lighter hatched areas are velocities measured by us; darker hatched are previous observations by others.

#### 4.2. Sky projection

In regard to the interpretation of data in three-dimensional redshift space, particularly in the absence of magnitude controls, the reader is directed to the introductory discussion in Section 3.2 of Paper I. In interpreting these plots, note that the Hydra–Antlia ZOA region is covered observationally as deep as the current Crux region, whereas other low-latitude regions only have very sparse redshift information

Figure 5 shows the surveyed region and its surrounding volume sliced in redshift intervals of  $\Delta v = 2000 \text{ km s}^{-1}$ . As already indicated, most of the data points, within the outlined Crux region, are from the new observations. Conspicuous features occur in the second and third slices - matching the excess already noted in the histogram of Figure 4.

In the second slice, the new data reinforce the presence of a narrow filamentary structure running all the way from  $\ell = 340^\circ$ ,  $b = -25^\circ$  to the Centaurus cluster at  $\ell = 303^\circ$ ,  $b = 20^\circ$ . This is believed to be part of a Great Wall-like structure seen edge-on – the Centaurus Wall. The new observations fill in a portion of this feature previously hidden by the Milky Way - as might be expected of a continuous massive structure. The break, due to the obscuration close to the galactic plane is now much narrower. The new data in the top-left corner of the Crux region is concentrated in the  $3500 - 4500 \text{ km s}^{-1}$  range - slightly closer than most other condensations within the wall. There are also indi-

cations of weaker filaments: One crosses north-south at  $\ell = 305^\circ$  while another passes just outside the south-east corner of the surveyed area.

However, the most important structure revealed by the present survey occurs in the third slice down. This is a concentration of galaxies centred at  $5000 \text{ km s}^{-1}$  in the upper (northern) segment of the surveyed volume. Together with the neighbouring galaxies outside the survey volume, it suggests a large-scale structure running more or less horizontally across the diagram. We have earlier labelled this structure as the “Norma supercluster” (Woudt et al. 1997). Traces can also be seen in the following slice, so the feature is also probably wall-like seen roughly side on - i.e. its width (or depth in Fig 5) being some  $3000 \text{ km s}^{-1}$  and its thickness several hundred  $\text{km s}^{-1}$  unless much is still hidden by the dense obscuration. We shall see however (in Fig 6) that this feature is more complex. For the moment note the concentration at  $\ell = 305^\circ$  in the fourth slice - coincident with that seen earlier in Figure 1. Bearing in mind its greater distance, compared to the Centaurus Wall mentioned above, this new structure must be similarly massive. The Norma cluster is situated where these two massive structures – the Centaurus Wall and the Norma supercluster – intersect.

Features at greater redshifts are understandably narrower in angular dimensions, and more difficult to discern: The fourth slice shows a feature running along the southern boundary of the Crux region. Beyond that, the data is generally too sparse, except for a weak concentration at  $14000 - 16000 \text{ km s}^{-1}$  in the south-east (bottom left), that corresponds to the relatively distant overdensity noted earlier.

#### 4.3. Pie diagrams

Our final set of plots, Figure 6, shows slices in galactic latitude; the uppermost including the Centaurus and Hydra clusters, the lowest the Pavo cluster.

The product of our survey appears as the middle slice, which would otherwise be largely blank. Instead, the slice reveals a cellular structure - familiar from plots elsewhere in the sky (eg Fairall et al. 1990) - but never before discerned so clearly at so low a galactic latitude. Presumably, the appearance is somewhat assisted by a favourable angle of cut. The cell sizes, and the voids so contained, are  $1000 - 2000 \text{ km s}^{-1}$  in diameter.

Of particular interest is a radial feature (from  $5300$  to  $7000 \text{ km s}^{-1}$ ), almost dead centre, that corresponds to the concentration at galactic longitude  $\ell = 305^\circ$ . The feature could be the “finger of God” of a small cluster except it is not discernable as such in a central longitude slice (not reproduced here).

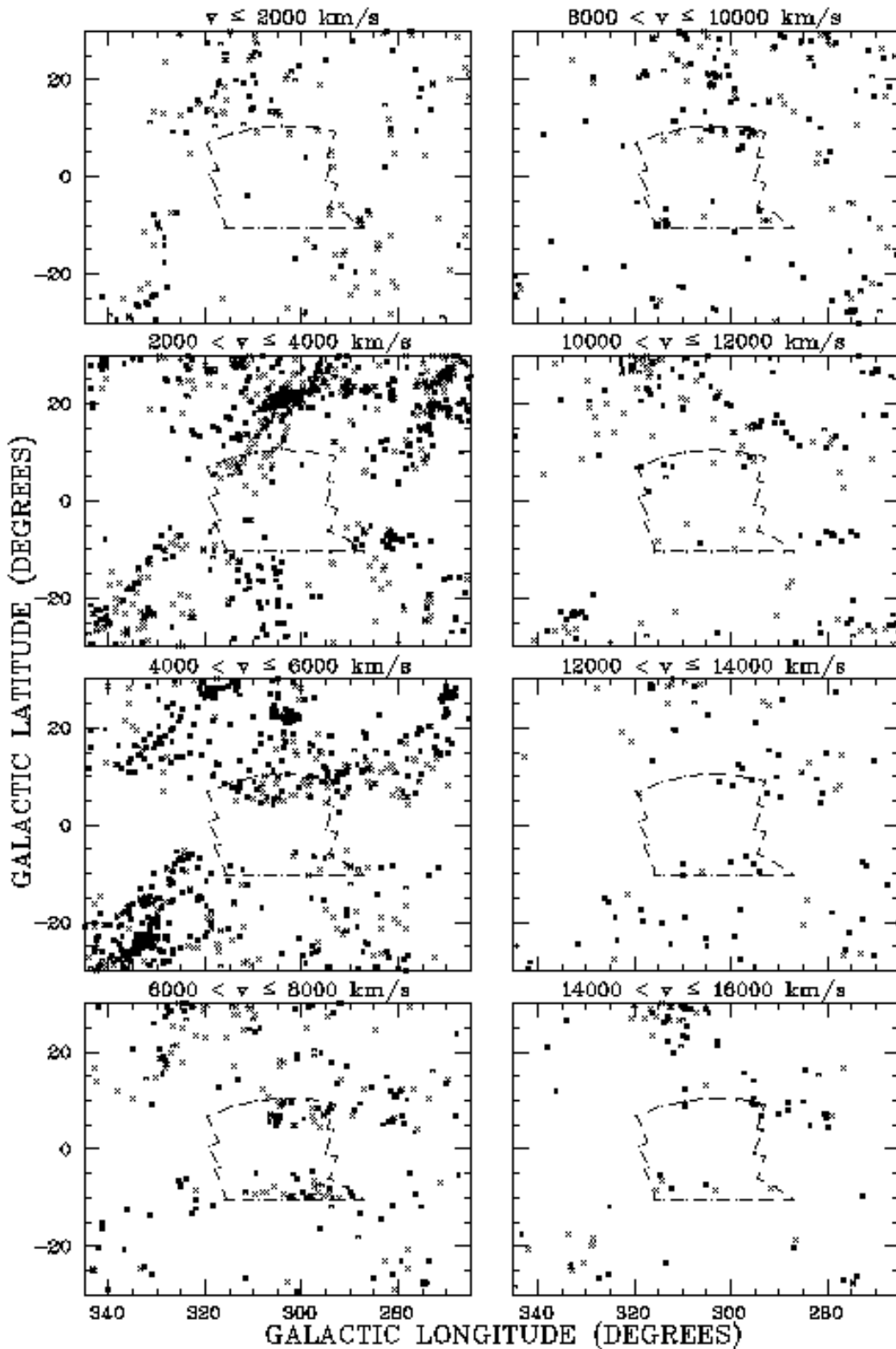


**Fig. 5.** Sky projections in galactic coordinates for redshift intervals of  $\Delta v = 2000 \text{ km s}^{-1}$ . Within the panels the redshifts are subdivided into intervals of  $\Delta v = 1000 \text{ km s}^{-1}$ : filled squares mark the nearer redshift interval (e.g.,  $v \leq 1000 \text{ km s}^{-1}$  in the top-left panel), crosses the more distant interval ( $1000 < v \leq 2000 \text{ km s}^{-1}$  in same panel). The skyplots increase in velocity-distance from the top-left panel to the bottom-right panel as marked above each panel. The area of our investigation is outlined.

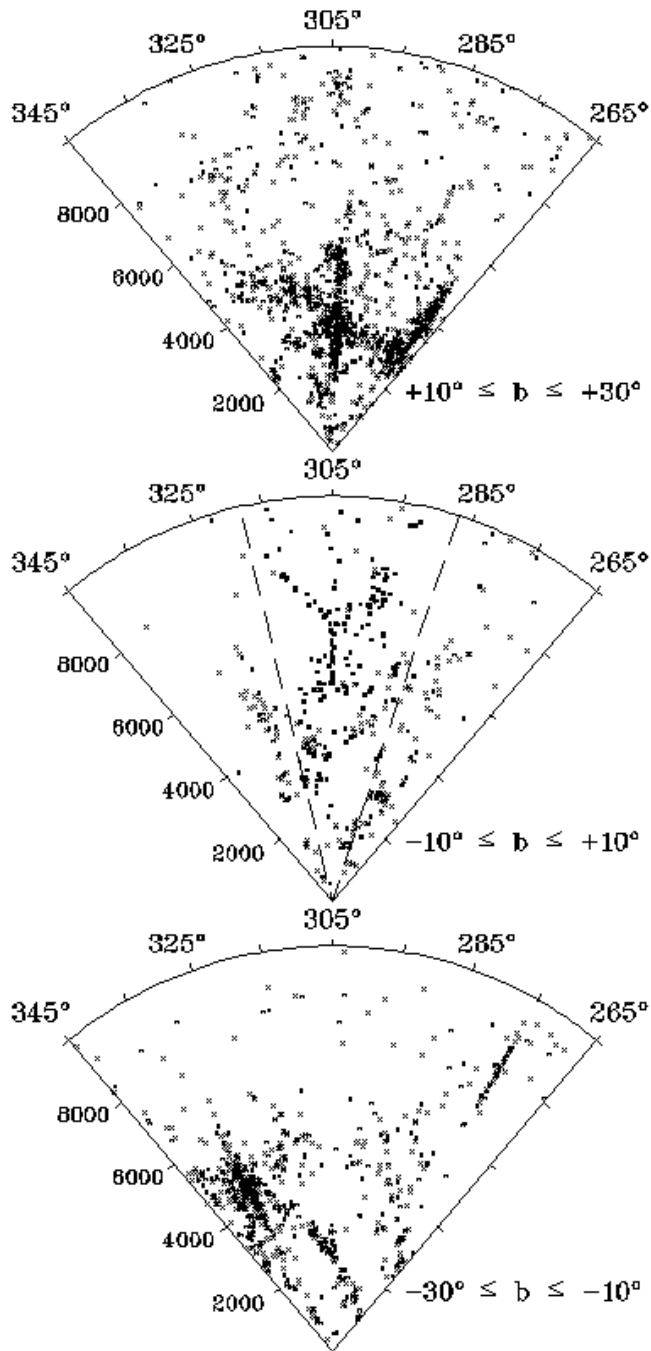


**Fig. 6.** Redshift slices out to  $v < 10000 \text{ km s}^{-1}$  for the longitude range  $265^\circ < \ell < 345^\circ$ . The top panels display the structures above the GP ( $+10^\circ \leq b \leq +30^\circ$ ) the middle panel in the GP ( $-10^\circ \leq b \leq +10^\circ$ ) and the bottom panel the structures below the GP ( $-30^\circ \leq b \leq -10^\circ$ ). The dashed lines in the middle panel delimits the survey area. Filled squares are measurements from the SAAO, crosses from the literature.

## 5. Summary.

The main finding of this survey has been an overdensity of galaxies in the  $3000 - 8000 \text{ km s}^{-1}$  range in redshift. Rather than a single feature, this overdensity represents a set of distinct cellular structures similar to those seen at higher galactic latitudes and for which Figure 6 (middle plot) provides a mapping. The survey also provides more detailed mapping of the “Centaurus Wall” where it crosses the Milky Way.

*Acknowledgements.* The authors would like to thank the night assistants Francois van Wyk and Fred Marang as well as the staff at the SAAO for their hospitality. APF and PAW are supported by the South African FRD. The research by RCKK is being supported with an EC-grant. Financial support was provided by CNRS through the Cosmology GDR program. This research has made use of the NASA/IPAC Extragalactic Database (NED), which is operated by the Jet Propulsion Laboratory, Caltech, under contract with the National Aeronautics and Space Administration.

## References

- Dressler, A. 1991, ApJS 75, 241
- Fairall, A.P. 1983, MNRAS 203, 47
- Fairall, A.P., Palumbo, G.G.C., Vettolani, G., et al. 1990, MNRAS 247, 21P
- Fairall, A.P., Paverd, W.R. 1995 in “Wide-Field Spectroscopy and the Distant Universe”, eds. S.J. Maddox and A. Aragon-Salamanca, World Scientific, Singapore, 121
- Fairall, A.P. 1996, the Southern Redshift Catalogue, maintained at the University of Cape Town (available from fairall@uctvms.uct.ac.za)
- Felenbok, P., Guérin, J., Fernandez, A., et al. 1997, Experimental Astronomy, in press
- Fisher, K.B., Huchra, J.P., Strauss, M.A., et al. 1995, ApJS 100, 69
- Huchtmeier, W.K., Richter O.-G. 1989, The General Catalogue of HI-Observations of Galaxies, New York: Springer-Verlag
- Kolatt, T., Dekel, A., Lahav, O. 1995, MNRAS,
- Kraan-Korteweg, R.C., Fairall, A.P., Balkowski, C., 1995 (Paper I), A&A 297, 617
- Kraan-Korteweg, R.C., Woudt, P.A., Cayatte, V., et al. 1996 (KK96), Nature 379, 519
- Kraan-Korteweg, R.C., Fairall, A.P., Woudt, P.A., et al. 1996, A&A 315, 549
- Kraan-Korteweg, R.C. 1997 in preparation
- Lauberts,A. 1982, The ESO/Uppsala Survey of the ESO (B) Atlas, ESO: Garching
- Lynden-Bell, D., Faber, S.M., Burstein, D., et al. 1988, ApJ 326, 19
- Salem, C., Kraan-Korteweg, R.C. 1997 in preparation
- Strauss, M.A., Huchra, J.P., Davis, M., et al. 1992, ApJS 83, 29
- Vaucoleurs, G. de, Vaucoleurs, A. de, Corwin, H.G. 1976, Second Reference Catalogue of Bright Galaxies (RC2), University of Texas Press, Austin
- Visvanathan, N., van den Bergh, S. 1992, AJ 103, 1057
- Woudt, P.A., Kraan-Korteweg, R.C. 1997 (WKK97), in preparation

Woudt, P.A., Fairall, A.P., Kraan-Korteweg, R.C., 1997, in  
“Dark and Visible Matter in Galaxies and Cosmological Im-  
plications”, eds. M. Persic and P. Salucci, A.S.P. Conf.Ser.,  
in press.